THE JOURNAL OF PHYSICAL CHEMISTRY A

pubs.acs.org/JPCA Article

Unusual and Conventional Dative Bond Formation by s^2 Lone Pair Donation from Alkaline Earth Metal Atoms to BH_3, AlH_3, and GaH_3

Published as part of The Journal of Physical Chemistry virtual special issue "Emily A. Carter Festschrift".

Iwona Anusiewicz, Dawid Faron, Piotr Skurski, and Jack Simons*

Cite This: *J. Phys. Chem. A* 2020, 124, 5369–5377 Read Online

ACCESS | Metrics & More | Article Recommendations

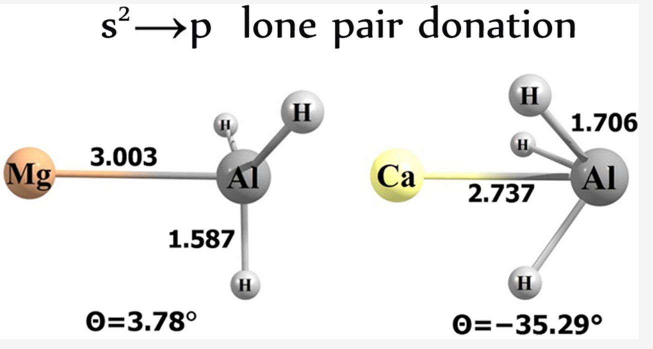

ABSTRACT: Using ab initio electronic structure methods with flexible atomic orbital basis sets, we examined the nature of the bonding arising from donation of an ns^2 electron pair on an alkaline earth atom (Mg or Ca) into a vacant n′p orbital on the group 13 atom of BH_3, AlH_3, or GaH_3. We also examined what happens when an excess electron is attached to form corresponding molecular anions. Although the geometries of $MgBH_3$, $MgAlH_3$, $MgGaH_3$, and $CaBH_3$ are found to be much as one would expect for datively bound molecules, $CaAlH_3$ and $CaGaH_3$ were found to have very unusual geometries in that their Al−H or Ga−H bonds are directed toward the Ca atom rather than away, as in the other compounds. Internal electrostatic Coulomb attractions between the partially positively charged Ca center and the partially negatively charged H centers were suggested as a source of these unusual geometries. The other novel finding is that the electron affinities (EAs) of all six $M'-MH_3$ species lie in the 0.7−1.0 eV range, which is suggestive of ionic electronic structures for the neutrals even though the partial charges on the alkaline earth centers are as low as 0.3 atomic units. Partial positive charge on the alkaline earth atoms combined with substantial electron affinities of the BH_3, AlH_3, and GaH_3 groups, but only when distorted from planar geometries, were suggested to be the primary contributors to the large EAs.

I. INTRODUCTION

The elements of group 13 of the periodic table comprising boron, aluminum, gallium, indium, and thallium form many compounds with hydrogen. In particular, boron is capable of forming various hydrides such as trihydridoboron, BH_3,[1] diborane (B_2H_6),[2] and decaborane ($B_{10}H_{14}$)[1] in some of which bridging three-center bonds occur. Aluminum and gallium form fewer stable hydrides (alane (AlH_3) and polymeric $(AlH_3)_n$ derivatives; gallane (GaH_3), digallane (Ga_2H_6), and $(GaH_3)_n$ polymeric compounds[1,3]) whereas the hydrides of indium and thallium are known mostly as fragments of complex compounds.[1,2,4] Certain hydrides of boron, aluminum, and gallium have attracted attention primarily due to their usefulness in synthesis and materials chemistry. For example, borane (BH_3) is a reaction intermediate in the pyrolysis of diborane (leading to higher boranes[1]), various boron hydrides are used as components in classical and secondary batteries and novel rechargeable storage systems[5−11] whereas alane (AlH_3) plays a reducing agent role in organic synthesis (as a selective reducer of many functional groups).[12] However, gallium hydrides are usually investigated in the context of properties exhibited by their adducts containing 4- or 5-coordinate gallium central atom(s) and involving GaH_3 and monodentate or bidentate ligands.[13,14] In addition, AlH_3 is a rocket fuel additive[15] while various polymeric hydrides of boron, aluminum, and gallium remain active candidates for storing hydrogen.

Due to the fact that earlier literature reports describing the possibility of an excess electron binding by borane, alane, and gallane were contradictory (for BH_3),[16−20] scarce and outdated (for AlH_3)[21,22] or absent (for GaH_3), we recently investigated the issue of the stability of BH_3^-, AlH_3^-, and GaH_3^- anions.[23] In the course of our ab initio studies (based on a CCSD(T)/aug-cc-pV5Z theoretical approach), we established the adiabatic electron affinity (EA) of BH_3 and the vertical electron detachment energy (VDE) of $(BH_3)^-$ to be 0.02 and 0.04 eV, respectively, and confirmed the planar D_{3h}-symmetry structure of both neutral BH_3 and its daughter BH_3^- anion.

Received: April 17, 2020
Revised: May 24, 2020
Published: June 4, 2020

Unlike BH_3^-, AlH_3^- and GaH_3^- were found to adopt nonplanar geometries and to bind an excess electron more strongly (the EAs of AlH_3 and GaH_3 were calculated to be 0.31 and 0.26 eV, respectively, while the VDEs of AlH_3^- and GaH_3^- were evaluated to be 0.41 and 0.37 eV, respectively).[23]

In our most recent paper,[24] we investigated compounds formed by an attachment of an alkaline earth metal atom (Be or Mg) to BH_3. We studied such a functionalization of the simplest borane mostly because we had become intrigued by the possibility of forming electronically stable anions by assembling two closed-shell species whose tendency to bind an excess negative charge is either zero (neither Be nor Mg forms a stable anion[25]) or tiny (BH_3).[23] Our calculations revealed that the molecules assembled from these species are capable of forming electronically and thermodynamically stable $BeBH_3^-$ and $MgBH_3^-$ anions whose equilibrium structures are similar to those of their corresponding $BeBH_3$ and $MgBH_3$ neutral parents. Also, we found that the values of adiabatic electron affinity (1.11 eV) and vertical electron detachment energy (1.30 eV) predicted for $BeBH_3^-$ anion are significant and larger than those obtained for the $MgBH_3^-$ anion (for which the EA of 0.68 eV and VDE of 0.74 eV were calculated). In addition, while investigating the structures of $BeBH_3$ and $MgBH_3$, we suggested that an alkaline earth metal atom forms a rather atypical bond with the boron atom. Namely, recalling that boron and its derivatives are well-known lone pair acceptors, we proposed to identify the Be−B and Mg−B bonds as dative bonds formed by the s^2 electron lone pair donation (coming from Be or Mg) to an empty 2p boron orbital of BH_3. Due to the unusual nature of these bonds, we discussed them in terms of the NBO analysis (which led to the 0.8287(2s)Be + 0.5597(2p)B and 0.8693(3s)Mg + 0.4943(2p)B hybrid composition for the bonds in $MgBH_3$ and $MgBH_3$, respectively) and concluded that the bonding effects in $BeBH_3$ and $MgBH_3$ are primarily the result of the overlap of doubly occupied 2s Be orbital or 3s Mg orbital and an empty 2p B orbital.

With the intention of gaining a better insight into the bonding in the systems formed by assembling alkaline earth metal atom and the hydrides of 13 group elements as well as characterizing the structural changes accompanying the formation of these compounds, in this contribution we provide the results of detailed considerations regarding the electronic and thermodynamic stability of $M'BH_3$, $M'AlH_3$, and $M'GaH_3$ (M′ = Mg, Ca) neutral molecules and their corresponding anions, established on the basis of correlated ab initio calculations using flexible atomic orbital basis sets.

II. METHODS

The equilibrium structures and corresponding harmonic vibrational frequencies of the closed-shell neutral MBH_3, $MAlH_3$, and $MGaH_3$ (M = Mg, Ca) molecules and their corresponding doublet anions were determined by applying the coupled-cluster method with single and double excitations (CCSD)[26−29] using the aug-cc-pVTZ basis set for Mg, B, Al, Ga, and H atoms[30] and the aug-cc-pVTZ-PP basis set for Ca.[31] The electronic energies of the systems studied were then refined by employing the coupled-cluster method with the single, double, and noniterative triple excitations (CCSD(T)) method[26−29] and the same basis sets. Both during the geometry optimizations followed by harmonic vibrational frequencies calculations with the CCSD method and while refining the electronic energies using the CCSD(T) method, all orbitals in the core and valence shells have been correlated. For all of the structures considered here, all vibrational frequencies were real other than for the transition states we briefly mention where one frequency was imaginary.

The vertical electron detachment energies of the anions and the adiabatic electron affinities (not including zero-point vibrational corrections) of the neutral species were calculated by employing the supermolecular approach (i.e., by subtracting the energy of the anion from that of the neutral) involving the CCSD(T)/aug-cc-pVTZ/aug-cc-pVTZ-PP energies and by applying the outer valence Green function OVGF method (*B* approximation)[32−40] together with the aug-cc-pVTZ and aug-cc-pVTZ-PP basis sets (again, all orbitals in the core and valence shells have been correlated during the OVGF calculations). Due to the fact that the OVGF approximation remains valid only for outer valence ionization for which the pole strengths (PS) are greater than 0.80−0.85,[41] we verified that the PS values obtained were sufficiently large to justify the use of the OVGF method (the smallest PS for the states studied in this work was equal to 0.905).

The partial atomic charges were evaluated by the natural bond orbital (NBO) analysis scheme[42−46] using the CCSD electron densities, and all calculations were performed with the GAUSSIAN16 (Rev. C.01) package.[47]

III. RESULTS

A. Geometries. When discussing the equilibrium structures of the neutral and anionic $M'-MH_3$ species (M′ = Mg or Ca; M = B, Al, Ga), we refer to an angle θ (defined in Figure 1) describing the deformation of the MX_3 fragment away from planarity. Positive values of θ are used to denote deformations in which the three M−H bonds are directed away from the alkaline earth atom and negative values of θ denote deformations in which the M−H bonds are directed toward the alkaline earth atom. It is the latter class of deformations that forms the unusual bonding paradigm referred to in our manuscript title; the former class constitutes the conventional paradigm.

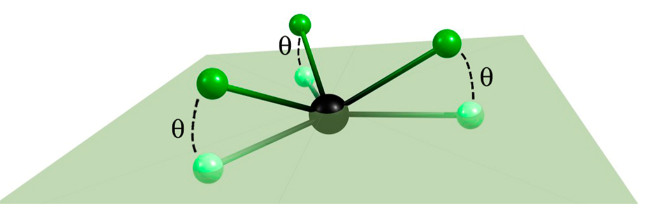

Figure 1. Definition of the θ angle that measures the distortion of the MH_3 unit's C_{3v}-symmetry (pyramidal) structure away from planarity.

A conventional dative bond involves donation of a lone electron pair from a Lewis base into an empty orbital of a Lewis acid as in, for example, H_3N-BH_3. In such cases, the planar Lewis acid undergoes a change in valence orbital hybridization from sp^2 (with an empty p orbital) toward sp^3, which thus gives rise to the distortion having positive θ. It is minimization of the electron repulsions between the donated partial electron pair and the M−H bonds' electrons that causes this change in hybridization. As we now demonstrate, there are additional electronic structure influences that come into play in some of the systems studied here that, for certain species, can produce forces that override these conventional hybridization factors and produce structures with negative θ values.

https://dx.doi.org/10.1021/acs.jpca.0c03432
J. Phys. Chem. A 2020, 124, 5369−5377

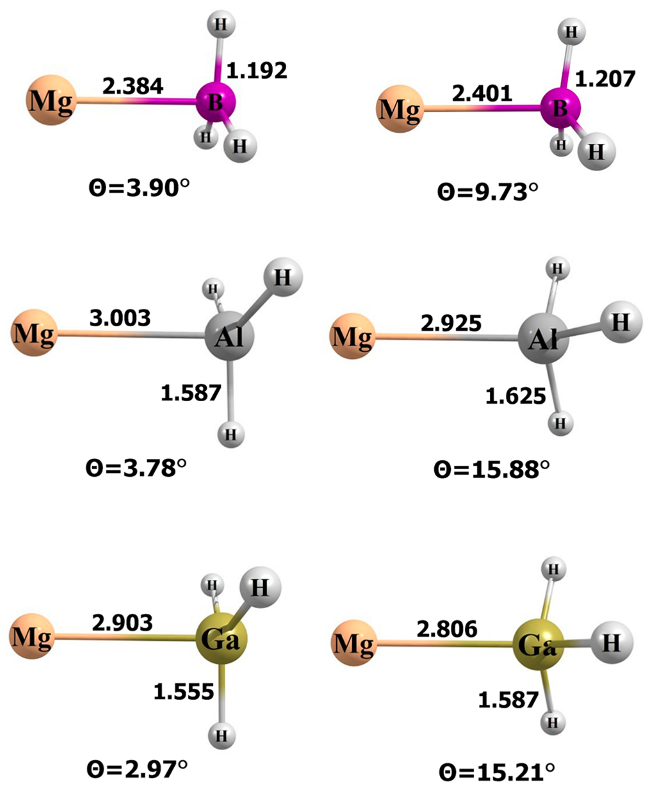

Figure 2. CCSD/aug-cc-pVTZ equilibrium structures (bond lengths in Å) of the neutral (left) and anionic (right) $MgMH_3$ (M = B, Al, Ga) systems.

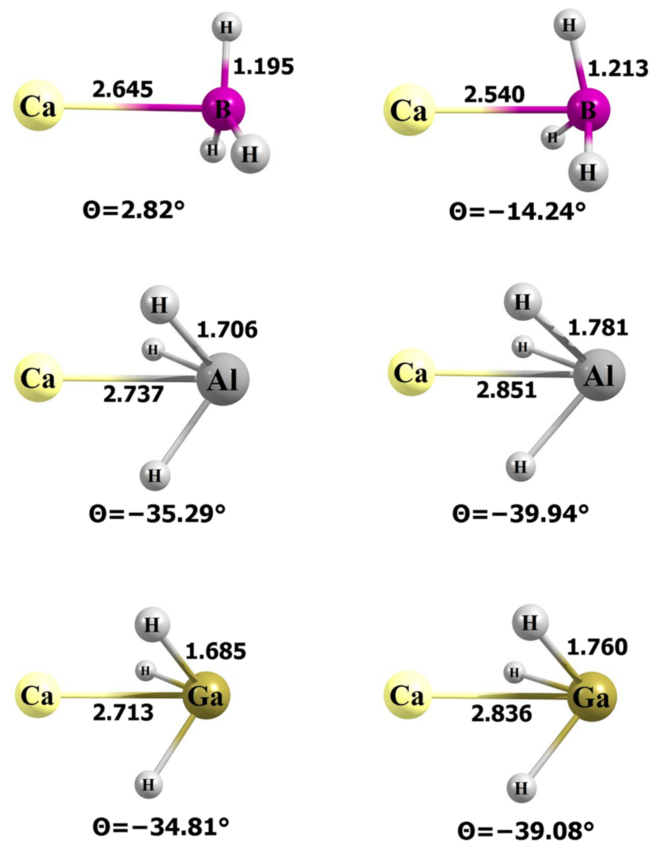

Figure 3. CCSD/aug-cc-pVTZ-PP equilibrium structures (bond lengths in Å) of the neutral (left) and anionic (right) $CaMH_3$ (M = B, Al, Ga) systems.

In Figures 2 and 3 we show the global minimum-energy structures we identified for the six species formed by bonding either Mg or Ca to BH_3, AlH_3, or GaH_3 along with the structures of the anions formed by adding one electron. In searching for the lowest energy structures, we did consider geometries such as H−Mg−AlH_2 but in all cases such structures were found to be considerably higher in energy than those discussed here. In ref 23 we studied the BH_3, AlH_3, and GaH_3 fragments and their anions and in ref 24 we studied Be and Mg bonded to BH_3 and the anions of these two complexes, and we will include some discussion of these species in the present work to offer comparisons. For some of the species, we also found higher energy local minima having θ values of opposite sign to those of our reported global minima. For example, for $MgAlH_3$ we found a negative θ local minimum 8 kcal/mol above our positive θ global minimum with a transition state 10 kcal/mol above the global minimum. For $CaAlH_3$ we found a positive θ local minimum 8 kcal/mol above our negative θ global minimum with a barrier 12 kcal/mol above the global minimum. We did not explore these minima more because they lie above or very close to the energies of M′ + AlH_3.

There are several features worth noting in these structures:

a. The most unusual feature occurs in $CaAlH_3$ and $CaGaH_3$ and in the $CaBH_3^-$, $CaAlH_3^-$, and $CaGaH_3^-$ anions and presents as negative values for the distortion angle θ; notice how the three B−H, Al−H, or Ga−H bonds bend toward rather than away from the Ca atom. The origin of this feature will be discussed in the next section.

b. In all of the other neutral and anionic species, the distortion angle θ is positive as it is in conventional Lewis acid−base acceptor−donor pairs such as H_3B−NH_3.

c. In all three of the Mg-containing species, the θ angle increases significantly in moving from the neutral to the anion.

d. In the Ca-containing species involving Al and Ga, the θ angle becomes more negative in moving from the neutral to the anion and for $CaBH_3$ it moves from positive θ to negative θ in moving to the anion.

e. For the neutral compounds containing B, the Mg−B or Ca−B bond lengths are very close to the sum of the B and Mg or Ca covalent radii[48] (0.84 Å for B, 1.41 Å for Mg and 1.76 Å for Ca). However, for the neutral compounds containing Mg and Al or Ga, the Mg to Al or Ga bond lengths are 0.3 Å or more longer than the sum of the covalent radii (1.21 Å for Al and 1.22 Å for Ga) while for the compounds containing Ca and Al or Ga, the Ca to Al or Ga bond lengths are at least 0.2 Å shorter than the sum of the covalent radii.

In the following sections, we will attempt to interpret these observations especially those involving the unusual bonding paradigm involving negative θ angles.

B. Probable Origin of Unusual Structures. To understand why $CaAlH_3$ and $CaGaH_3$ (and their anions as well as the $CaBH_3^-$ anion) adopt the unusual geometries having negative θ values shown in Figures 2 and 3, let us examine the atomic partial charges extracted from our CCSD-level

https://dx.doi.org/10.1021/acs.jpca.0c03432
J. Phys. Chem. A 2020, 124, 5369−5377

calculations using the natural bond orbital method of Weinhold and co-workers.[42−46] We will first focus on the six neutral molecules and then consider what happens when an extra electron is added. In Table 1 we show the atomic charges

Table 1. Partial Atomic Charges (in au) Calculated for BH_3, AlH_3, and GaH_3 by Employing the NBO Population Analysis Using CCSD Electron Densities

system	atom	atomic charges
BH_3	B	0.354
	H	−0.118
AlH_3	Al	1.236
	H	−0.412
GaH_3	Ga	0.984
	H	−0.328

for the three electron acceptor MH_3 units in the absence of any alkaline earth atom and then we will compare these charge densities to those when the Mg or Ca atom is added.

Keeping in mind that H is slightly more electronegative than B, it is not surprising that the H atoms in BH_3 are slightly negatively charged. However, H is considerably more electronegative than Al or Ga as a result of which the H atoms in AlH_3 and GaH_3 are quite negatively charged. Also, keep in mind that BH_3 is a very poor electron acceptor (having an EA near zero) while AlH_3 and GaH_3 have modest EAs (near 0.3 eV).

Now, let us see what happens to the atomic charges on the MH_3 units' atoms when an Mg or Ca atom is attached. In Table 2 we show the partial atomic charges for the six M′−

Table 2. NBO Partial Atomic Charges (in au) Calculated Using CCSD Electron Densities for Mg−MH_3 and Ca−MH_3 and Changes in Charges (Δq) on MH_3 Atoms When Mg or Ca Is Added (for Neutral)

species	atom	atomic charges	Δq
$MgBH_3$	Mg	0.503	
	B	−0.309	Δq(B) = −0.66
	H	−0.065	Δq(H) = +0.05
$MgAlH_3$	Mg	0.300	
	Al	0.854	Δq(Al) = −0.38
	H	−0.385	Δq(H) = +0.03
$MgGaH_3$	Mg	0.326	
	Ga	0.549	Δq(Ga) = −0.44
	H	−0.292	Δq(H) = +0.04
$CaBH_3$	Ca	0.613	
	B	−0.405	Δq(B) = −0.76
	H	−0.069	Δq(H) = +0.05
$CaAlH_3$	Ca	0.975	
	Al	0.453	Δq(Al) = −0.78
	H	−0.476	Δq(H) = −0.06
$CaGaH_3$	Ca	0.996	
	Ga	0.257	Δq(Ga) = −0.73
	H	−0.418	Δq(H) = −0.09

MH_3 species (central column) as well as the differences (right column) between these atomic charges and those shown in Table 1 for the bare MH_3 units.

There are several features to note in these data:

a. There are only minor changes in the charges on the three H atoms when either an Mg or Ca atom is attached to BH_3, AlH_3, or GaH_3. As a result, the H atoms remain only weakly negatively charged in the BH_3-containing species but are still quite negatively charged in the AlH_3- and GaH_3-containing species.

b. Most of the changes in atomic charges occur at the alkaline earth and B, Al, or Ga atoms and result from electron density flow from the ns^2 lone pair on the alkaline earth atom to the B, Al, or Ga atom. Of course, this is not surprising and the donor → acceptor electron pair donation phenomenon is expected in such cases.

c. The donor → acceptor bond formation renders B negative in the first and fourth compounds but leaves Al or Ga positively charged in the other compounds.

d. The magnitude of the electron density flow is considerably larger in the Ca-containing species than in the Mg-containing species especially when the MH_3 unit contains Al or Ga; this likely reflects the considerable difference in the two atoms' ionization potentials (7.6 eV for Mg and 6.1 eV for Ca).

On the basis of these atomic partial charges, we suggest the following reason behind the unusual (i.e., negative θ values) geometries found for neutral $CaAlH_3$ and $CaGaH_3$. In these two cases, there exist very strong Coulomb stabilization energies acting to attract the alkaline earth atom toward the

Table 3. Coulombic Interaction Energies Computed from Eq 1 Using the Atomic Partial Charges Given in Table 2

species	M′−H distance (Å)	Coulombic energy (eV)
$MgBH_3$	2.737	−0.52
$MgAlH_3$	3.488	−1.43
$MgGaH_3$	3.364	−1.22
$CaBH_3$	2.955	−0.62
$CaAlH_3$	2.238	−8.96
$CaGaH_3$	2.255	−7.98

three equivalent H atoms. To illustrate this point in Table 3, we show the Coulombic energies computed as

$$C = \sum_{J=1}^{3} \frac{14.4 q_{H_J} q_{M'}}{R_{M'-H_J}} \text{ eV} \quad (1)$$

where $R_{M'-H_J}$ is the distance in Å from the alkaline earth atom M′ to the Jth H atom and $q_{M'}$ and q_{H_J} are the partial charges on these atoms, respectively.

Clearly, the cases of $CaAlH_3$ and $CaGaH_3$ are unique in the size of the Coulomb energies. We suggest it is these strong interatomic attractions that give rise to the unusual (negative θ) geometries observed in these two cases. For the other four species, there certainly are non-negligible Coulomb attractions between the alkaline earth atoms and the H atoms. However, it appears that these attractions are not strong enough to overcome the influence of the dative bond between the alkaline earth atom and the B, Al, or Ga atom. As explained earlier, this kind of conventional donor → acceptor bonding acts to rehybridize the B, Al, or Ga atom away from sp^2 toward sp^3 hybridization and thus to positive θ.

It might occur to the reader that some other influence is giving rise to the negative θ geometries and that the large partial charges then arise from that influence. However, we do not believe this is the case; we think it is the large partial

https://dx.doi.org/10.1021/acs.jpca.0c03432
J. Phys. Chem. A 2020, 124, 5369−5377

charges that cause the negative θ values, and we base this opinion on two observations:

1. From Table 1 we see that the partial charges on the H atoms of AlH_3 and GaH_3 are already (i.e., in their planar geometries with no Mg or Ca atom attached) quite substantial (−0.3 to −0.4), and we see from Table 2 that they increase in magnitude very little when a Mg or Ca atom is attached and the geometry evolves to negative θ. So, there is no evidence that the charges that we claim give rise to the large Coulomb attractions become large as θ evolves to negative values; they already were large and changed little as θ varied.
2. From Table 2 we also see that the partial charges on the Ca atoms in $CaAlH_3$ and $CaGaH_3$ are much higher than in the other species. It appears that a combination of the already-existing large negative charges on the H atoms of AlH_3 and GaH_3 and the large positive charges on the Ca atoms in $CaAlH_3$ and $CaGaH_3$ are what brings these two species into the realm of negative θ. Certainly, for the other four species, attractive Coulomb interactions between the Mg or Ca atom and the three H atoms in the MH_3 unit exist (see Table 3) but these interactions are not sufficient to overcome the tendency of Lewis acid−base pairs to adopt the positive θ geometries.

C. Stability with Respect to Fragmentation. We also examined how stable the six Lewis base−acid complexes are toward dissociation into various fragments. In Table 4, we present the results of such studies.

For all six molecules, breaking apart into M′ + MH_3 is the least endergonic with ΔG^{298} values ranging from 2 to 13 kcal/mol; so these species are not very strongly bound even though there exists strong intramolecular Coulomb stabilizations. However, all six molecules are substantially more stable with respect to dissociation into either $M'H_2$ + MH or M′MH + H_2.

Table 4. Gibbs Free Energies (ΔG^{298} in kcal/mol) Predicted for the Fragmentation Processes of the Neutral Systems by Using the CCSD(T)/aug-cc-pVTZ/aug-cc-pVTZ-PP Electronic Energies Including Zero-Point Energy Corrections, Thermal Corrections, and Entropy Contributions (at T = 298.15 K) Calculated at the CCSD/aug-cc-pVTZ/aug-cc-pVTZ-PP Level

fragmentation path	ΔG^{298}
$MgBH_3 \rightarrow Mg + BH_3$	7.08
$MgBH_3 \rightarrow MgBH + H_2$	112.09
$MgBH_3 \rightarrow MgH_2 + BH$	85.67
$MgAlH_3 \rightarrow Mg + AlH_3$	2.30
$MgAlH_3 \rightarrow MgAlH + H_2$	21.67
$MgAlH_3 \rightarrow MgH_2 + AlH$	77.04
$MgGaH_3 \rightarrow Mg + GaH_3$	3.55
$MgGaH_3 \rightarrow MgGaH + H_2$	23.54
$MgAlH_3 \rightarrow MgH_2 + GaH$	160.84
$CaBH_3 \rightarrow Ca + BH_3$	11.75
$CaBH_3 \rightarrow CaBH + H_2$	71.75
$CaBH_3 \rightarrow CaH_2 + BH$	154.25
$CaAlH_3 \rightarrow Ca + AlH_3$	13.25
$CaAlH_3 \rightarrow CaAlH + H_2$	27.37
$CaAlH_3 \rightarrow CaH_2 + AlH$	151.90
$CaGaH_3 \rightarrow Ca + GaH_3$	10.93
$CaGaH_3 \rightarrow CaGaH + H_2$	25.69
$CaGaH_3 \rightarrow CaH_2 + GaH$	232.12

In our earlier work,[24] we found that $BeBH_3$ dissociating into Be + BH_3 had a ΔG^{298} of 10.68 kcal/mol.

D. Negative Ions. We also examined what happens when an excess electron is added to these six species to form molecular anions. Recall that the Mg and Ca atoms have zero and very small (0.04 eV) EAs, respectively, and that the EAs of BH_3 (ca. 0 eV), AlH_3 (0.3 eV), and GaH_3 (0.3 eV) are also quite small. Nevertheless, the EAs and vertical electron detachment energies (VDEs) of the six molecules studied here turn out to be substantial, as shown in Table 5.

Table 5. Adiabatic Electron Affinities (EA in eV Not Including Zero-Point Energy Corrections) of the Neutral Systems and Vertical Electron Detachment Energies (VDE in eV) of Their Corresponding Anions Calculated at the CCSD(T)/aug-cc-pVTZ/aug-cc-pVTZ-PP Level (EA) and OVGF/aug-cc-pVTZ/aug-cc-pVTZ-PP Level (VDE) for the Equilibrium Structures Obtained by Employing the CCSD/aug-cc-pVTZ/aug-cc-pVTZ-PP Theoretical Approach

	EA	VDE
$MgBH_3/(MgBH_3)^-$	0.675	0.914
$MgAlH_3/(MgAlH_3)^-$	0.930	1.206
$MgGaH_3/(MgGaH_3)^-$	0.865	1.227
$CaBH_3/(CaBH_3)^-$	0.811	1.001
$CaAlH_3/(CaAlH_3)^-$	0.989	1.295
$CaGaH_3/(CaGaH_3)^-$	0.991	1.332

The fact that the EAs of the AlH_3- and GaH_3-containing compounds have EAs and VDEs ca. 0.2−0.3 eV larger than the BH_3-containing compounds likely relates to the fact that AlH_3 and GaH_3 have EAs about this same amount larger than the EA of BH_3.

Having found such large EAs for all of these molecules, we wanted to understand the origin of this outcome. Earlier,[49] we had observed that EAs of donor → acceptor complexes could be altered by varying the degree of electron density flow from the donor to the acceptor. In those cases, the electron binding occurred at the positive (donor) end of the complex and the magnitude of the resulting EA was small and characteristic of dipole binding. However, the data shown in Table 5 do not support a similar perspective in these cases since the EAs are larger than is typical for dipole binding (e.g., ca. 0.1 eV); in fact, they are more similar to the EAs found for ionic molecules such as NaCl whose EA[50] is 0.727 eV.

To further search for the origins of the large EAs, we evaluated the atomic charge densities for the six anions using the same approach as discussed earlier and compared these charges to those in the corresponding neutral species. The point of this comparison was to consider where the excess electron's density accumulated and to perhaps understand why. The results are shown in Table 6.

Keep in mind that the atomic charge differences reflected in comparing the third and fifth columns of Table 6 result from the charge density of the anion's SOMO as well as changes in the other occupied orbitals accompanying addition of the electron. There are several things worth noting in these data:

a. For the first four compounds, adding an electron renders the alkaline earth atom essentially neutral while for the last two species the Ca atom remains highly positively charged. Considering the substantial ionization potentials of Mg (7.6 eV) and Ca (6.1 eV), adding electron density to the partially positively charged Mg or Ca

Table 6. NBO Partial Atomic Charges Calculated Using CCSD Electron Densities for Neutral and Anion Species as Well as the Changes in Charges in Moving from the Neutral to the Anion

system	atom	neutral charges	atom	anion charges	Δq
$MgBH_3$	Mg	+0.503	Mg	+0.072	−0.431
	B	−0.309	B	−0.820	−0.511
	H	−0.065	H	−0.084	−0.019
$MgAlH_3$	Mg	+0.300	Mg	+0.036	−0.264
	Al	+0.854	Al	+0.194	−0.660
	H	−0.385	H	−0.410	−0.025
$MgGaH_3$	Mg	+0.326	Mg	+0.085	−0.241
	Ga	+0.549	Ga	−0.140	−0.689
	H	−0.292	H	−0.315	−0.023
$CaBH_3$	Ca	+0.613	Ca	+0.058	−0.555
	B	−0.405	B	−0.680	−0.275
	H	−0.069	H	−0.126	−0.057
$CaAlH_3$	Ca	+0.975	Ca	+0.789	−0.186
	Al	+0.453	Al	−0.046	−0.499
	H	−0.476	H	−0.581	−0.115
$CaGaH_3$	Ca	+0.996	Ca	+0.766	−0.230
	Ga	+0.257	Ga	−0.166	−0.423
	H	−0.418	H	−0.534	−0.125

centers could be one contribution to the EAs of the M′-MH_3 compounds.

b. Both the alkaline earth atoms and the group 13 atoms undergo substantial charge reductions while each of the three H atoms increase little (<0.1) in negative charge, and the group 13 atom gains negative charge even when it was already negatively charged in the neutral molecule prior to addition of the excess electron (e.g., as in $MgBH_3$ and in $CaBH_3$).

The latter observation in particular tells us that it is not the electrostatic potential existing within the neutral species that determines where the excess electron's density will accumulate because the partially negatively charged B atom becomes more negatively charged when an electron is added. So, we decided to examine the spatial distribution of the anions' SOMOs realizing that these orbitals strongly effect where the excess electron's density accumulates. In so doing, it is important to keep in mind that each SOMO is constrained to be orthogonal to all of its anion's underlying molecular orbitals.

In Figures 4 and 5 we show the HOMOs of the six neutrals as well as the SOMOs of the corresponding anions.

Before discussing the SOMOs, it is useful to analyze the spatial distributions and nodal patterns of the six HOMOs to which the corresponding SOMOs must be orthogonal.

For the first four species:

a. The NBO analyses reveal that these four HOMOs consist (almost entirely) of Mg−M or Ca−M (M = B, Al, Ga) bonding hybrids with orbital occupancies approaching 2 e, namely: $0.8980(3s)_{Mg} + 0.4399(2p)_{B}$ (for $MgBH_3$), $0.9369(3s)_{Mg} + 0.3497(3p)_{Al}$ (for $MgAlH_3$), $0.9302(3s)_{Mg} + 0.3670(4p)_{Ga}$ (for $MgGaH_3$), and $0.8891(4s)_{Ca} + 0.4577(2p)_{B}$ (for $CaBH_3$).

b. In addition, these bonding hybrids have orbital amplitudes centered on the three H atoms having the opposite sign as the alkaline earth ns orbital (also reflecting amplitude from the lobe of the group 13 p orbital directed away from the alkaline earth atom).

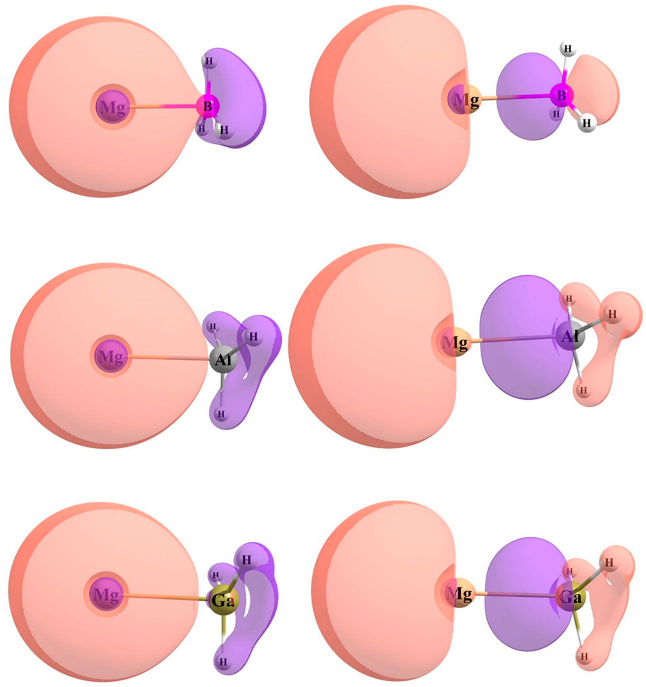

Figure 4. HOMO (for the neutral, left) and SOMO (for the anion, right) orbitals of the $MgMH_3$ (M = B, Al, Ga) systems.

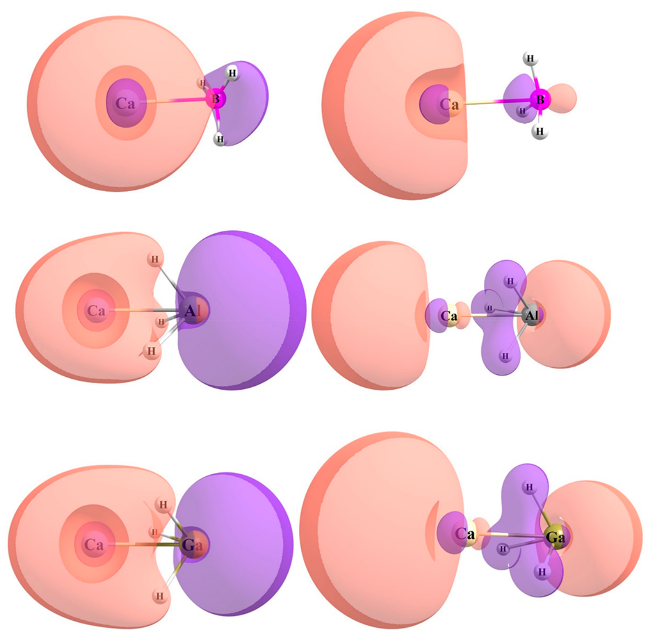

Figure 5. HOMO (for the neutral, left) and SOMO (for the anion, right) orbitals of the $CaMH_3$ (M = B, Al, Ga) systems.

For the two remaining species, we note that there are clear differences in comparison to the first four molecules:

a. The HOMOs consist largely of Ca 4s orbitals combined in a bonding manner with orbitals on the three H atoms.

b. Al or Ga orbital amplitude localized away from the Ca atom. Because of the negative θ values in these two species, this amplitude might be assigned to an sp^3 type hybrid orbital on the group 13 atom that has its major lobe directed away from the Ca atom and has its minor lobe directed toward the Ca atom and with a sign

https://dx.doi.org/10.1021/acs.jpca.0c03432
J. Phys. Chem. A 2020, 124, 5369−5377

consistent with bonding between the minor lobe and the Ca atom.

c. The NBO analysis describes these HOMOs as follows: The HOMO for $CaAlH_3$ is $0.848(3p)_{Al}$ lone pair and $0.529(LV(s))_{Ca}$ lone vacant orbital; for $CaGaH_3$ the HOMO is $0.831(4p)_{Ga}$ lone pair and $0.556(LV(s))_{Ca}$ lone vacant orbital. So, in both cases, the HOMO appears to be more of a lone pair type orbital that has amplitudes on both the Ca and group 13 atoms.

The qualitative differences between the HOMOs of the first four and latter two species is also consistent with the differences in internal Coulomb interactions discussed earlier as suggested sources of the negative θ values present in the latter.

Turning now to the anions' SOMOs, we note the following:

a. All six SOMOs have one more node along the C_{3v} axis than do the corresponding HOMOs; this reflects the fact that the SOMOs are orthogonal to the HOMO.
b. For the first four compounds, the SOMO has most of its amplitude on the side of the Mg or Ca atom directed away from the group 13 atom.
c. The SOMO of $CaBH_3^-$ is more similar to the SOMOs of the Mg-containing species than it is to the SOMOs of $CaAlH_3^-$ and $CaGaH_3^-$. We had anticipated that the SOMO of $CaBH_3^-$ would help us understand why this anion displays a (small) negative θ value while all of the Mg-containing species and their anions have positive θ values, but this anticipation was negated. However, we will have more to say about this issue below.
d. For the $CaAlH_3^-$ and $CaGaH_3^-$ SOMOs much of their amplitudes is localized outside the intermetal region to the left of the Ca atom and to the right of the Al or Ga atom.

Recall that the issues we are attempting to understand are why the $M'MH_3$ species have large EAs and what causes the $CaBH_3^-$ anion to have a negative θ value. Earlier, we pointed out that, for the first four species, the partially positively charged Mg or Ca atom is rendered essentially uncharged when the excess electron is added, and we suggested this was likely one contribution to the large EAs of these molecules. To uncover an additional likely contribution, we re-examined BH_3, AlH_3, and GaH_3. As noted earlier, these molecules have EAs in the 0.0−0.3 eV range and their anions have VDEs[23] between 0.02 and 0.4 eV, all of which are quite small. However, if the geometries of these species are distorted to assume nonzero θ values, the VDEs increase drastically, as shown in ref 23. To illustrate, we calculated the VDE of BH_3^- at $\theta = -14°$ (and using bonds lengths as in $CaBH_3^-$) and obtained 0.28 eV. Doing likewise for AlH_3^- and GaH_3^- at $\theta = -40°$ we obtained VDEs of 2.4 and 2.9 eV, respectively. Therefore, we suggest that a second contribution to the large EAs observed for all six compounds is likely the large VDEs of the highly distorted (i.e., having large negative θ values) AlH_3^- and GaH_3^- units occurring in $CaAlH_3^-$ and $CaGaH_3^-$.

In summary, for all six compounds there are two sites that offer strong electron attraction potential: the partially positively charged Mg^{q+} or Ca^{q+} site and the distorted BH_3, AlH_3, or GaH_3 site. For all species but $CaBH_3$, more of the added electron's density ends up on the group 13 atom even when the alkaline earth site is quite positively charged as it is in $CaAlH_3$ and $CaGaH_3$ (where the Ca charge is ca. 1.0) and even when the group 13 atom is already negatively charged as in $MgBH_3$ and $CaBH_3$. It is the spatial distribution of the anions' SOMOs and the fact that the SOMOs have to be orthogonal to the other orbitals that reflect where the extra electron's density ends up. Any electron density added to the MH_3 site's M atom tends to increase the magnitude of that site's θ value because the MH_3^- anions' VDEs increase with increasing $|\theta|$ which is why $CaAlH_3^-$ and $CaGaH_3^-$ have larger negative θ values than do their respective neutrals. The one character for which we do not yet have a reasonable explanation is why $CaBH_3^-$ has a negative θ value while its neutral has a positive θ.

In addition to finding that the anions studied here have large VDEs, it is also interesting to point out the substantial differences in the stabilities of the anions with respect to dissociation when compared to the neutrals, as shown in Table 7.

Table 7. Gibbs Free Energies (ΔG^{298} in kcal/mol) for Neutral and Anionic Systems Evaluated As Detailed in Table 4

	ΔG^{298}
$MgBH_3 \rightarrow Mg + BH_3$	7.08
$MgAlH_3 \rightarrow Mg + AlH_3$	2.30
$MgGaH_3 \rightarrow Mg + GaH_3$	3.55
$CaBH_3 \rightarrow Ca + BH_3$	11.75
$CaAlH_3 \rightarrow Ca + AlH_3$	13.25
$CaGaH_3 \rightarrow Ca + GaH_3$	10.93
$MgBH_3^- \rightarrow Mg + BH_3^-$	24.26
$MgAlH_3^- \rightarrow Mg + AlH_3^-$	15.60
$MgGaH_3^- \rightarrow Mg + GaH_3^-$	17.41
$CaBH_3^- \rightarrow Ca + BH_3^-$	29.42
$CaAlH_3^- \rightarrow Ca + AlH_3^-$	28.10
$CaGaH_3^- \rightarrow Ca + GaH_3^-$	27.61

Notice that all of the anions are much more stable with respect to dissociation into the donor/acceptor pairs than are the neutrals. This is a result of the quite large EAs of the neutral donor → acceptor molecules compared to the EAs of their corresponding donor and acceptor fragments.

IV. CONCLUSIONS

On the basis of the CCSD(T)/aug-cc-pVTZ/aug-cc-pVTZ-PP and OVGF/aug-cc-pVTZ/aug-cc-pVTZ-PP calculations performed for the $M'BH_3$, $M'AlH_3$, and $M'GaH_3$ neutral molecules and their corresponding anions (whose equilibrium structures were obtained at the CCSD/aug-cc-pVTZ/aug-cc-pVTZ-PP level of theory), we arrive at the following conclusions:

1. $M'-MH_3$ (M′ = Mg or Ca; M = B, Al, or Ga) forms rather weak dative bonds connecting the alkaline earth and group 13 atoms (ΔG^{298} for dissociation ranges from 2.3 to 13.25 kcal/mol). The ΔG^{298} values for dissociation of the corresponding anions are considerably larger.
2. The bonds are stronger for Ca-containing compounds than for Mg-containing compounds, probably because Ca is a better electron pair donor than Mg (i.e., Ca has a lower ionization potential than Mg).
3. The bonds involve donation of an ns^2 electron pair on the alkaline earth atom into an empty n′p orbital on the group 13 atom for $MgBH_3$, $MgAlH_3$, $MgGaH_3$, and

$CaBH_3$ and generate geometries with positive θ values (meaning the M−H bonds pucker away from the alkaline earth atom as expected).

4. For $CaAlH_3$ and $CaGaH_3$ the bonds seem to also involve considerable ionic character, which produces geometries with negative θ values (with the M−H bonds directed toward the alkaline earth atom) because the partially negatively charged H atoms are attracted to the partially positively charged Ca atom.
5. The distances between the alkaline earth and group 13 atoms are close to the sums of the covalent radii of the two atoms.
6. All six of the neutral species have large electron affinities (0.7−1.0 eV) and their anions have large vertical electron detachment energies (0.9−1.3 eV). As a result, and because the M′ and MH_3 fragments have very small EAs, the corresponding $M'{-}MH_3^-$ anions have much larger (positive) ΔG^{298} values for dissociation than do the $M'{-}MH_3$ neutrals.
7. Upon electron attachment to form the negative ions, small geometry changes take place except that the θ values become more negative for $CaAlH_3^-$ and $CaGaH_3^-$ and more positive for all the Mg-containing species and they evolve from slightly positive for neutral $CaBH_3$ to slightly negative for $CaBH_3^-$.
8. We suggest that it is a combination of the substantial partial positive charges on the alkaline earth atoms and the strong VDEs of the distorted (having nonzero θ values) BH_3^-, AlH_3^-, and GaH_3^- anions that give rise to the large EAs and VDEs observed for all six compounds.

■ AUTHOR INFORMATION

Corresponding Author

Jack Simons − *Henry Eyring Center for Theoretical Chemistry, Department of Chemistry, University of Utah, Salt Lake City, Utah 84112, United States*; orcid.org/0000-0001-8722-184X; Email: jack.simons@utah.edu

Authors

Iwona Anusiewicz − *Laboratory of Quantum Chemistry, Faculty of Chemistry, University of Gdańsk, 80-308 Gdańsk, Poland*; orcid.org/0000-0002-7506-8427

Dawid Faron − *Laboratory of Quantum Chemistry, Faculty of Chemistry, University of Gdańsk, 80-308 Gdańsk, Poland*

Piotr Skurski − *Laboratory of Quantum Chemistry, Faculty of Chemistry, University of Gdańsk, 80-308 Gdańsk, Poland; Henry Eyring Center for Theoretical Chemistry, Department of Chemistry, University of Utah, Salt Lake City, Utah 84112, United States*

Complete contact information is available at: https://pubs.acs.org/10.1021/acs.jpca.0c03432

Notes

The authors declare no competing financial interest.

■ ACKNOWLEDGMENTS

This research was supported by the Polish Ministry of Science and Higher Education grant No. DS 531-T110-D499-20. The calculations have been carried out using resources provided by Wroclaw Centre for Networking and Supercomputing (http://wcss.pl) grants No. 435 and 455. J.S. thanks the University of Utah Chemistry Department and Henry Eyring Center for Theoretical Chemistry for continued support and Professor Mark Gordon for useful suggestions.

■ REFERENCES

(1) Greenwood, N. N.; Earnshaw, A. *Chemistry of the Elements* (2nd ed.); Butterworth-Heinemann, 1997.

(2) Harding, C. J.; Johnson, D.; Janes, R. *Elements of the p block*; The Open University: Cambridge, UK, 2002; p 113.

(3) Wiberg, E.; Wiberg, N.; Holleman, A. F. *Inorganic chemistry*; Academic Press: San Diego, 2001.

(4) Cole, M. L.; Hibbs, D. E.; Jones, C.; Smithies, N. A. Phosphine and phosphido indium hydride complexes and their use in inorganic synthesis. *J. Chem. Soc., Dalton Trans.* **2000**, 545−550.

(5) Zhang, S. S. $LiBF_3Cl$ as an alternative salt for the electrolyte of Li-ion batteries. *J. Power Sources* **2008**, *180*, 586−590.

(6) Liu, H.; Tang, D. The effect of nanolayer AlF_3 coating on $LiMn_2O_4$ cycle life in high temperature for lithium secondary batteries. *Russ. J. Electrochem.* **2009**, *45*, 762−764.

(7) Li, J.; Zhang, Y.; Li, J.; Wang, L.; He, X.; Gao, J. AlF_3 coating of $LiNi_{0.5}Mn_{1.5}O_4$ for high-performance Li-ion batteries. *Ionics* **2011**, *17*, 671−675.

(8) Takahashi, K.; Hattori, K.; Yamazaki, T.; Takada, K.; Matsuo, M.; Orimo, S.; Maekawa, H.; Takamura, H. All-solid-state lithium battery with $LiBH_4$ solid electrolyte. *J. Power Sources* **2013**, *226*, 61−64.

(9) Silvestri, L.; Farina, L.; Meggiolaro, D.; Panero, S.; Padella, F.; Brutti, S.; Reale, P. Reactivity of Sodium Alanates in Lithium Batteries. *J. Phys. Chem. C* **2015**, *119*, 28766−28775.

(10) Teprovich, J. A.; Zhang, J.; Colón-Mercado, H.; Cuevas, F.; Peters, B.; Greenway, S.; Zidan, R.; Latroche, M. Li-Driven Electrochemical Conversion Reaction of AlH_3, $LiAlH_4$, and $NaAlH_4$. *J. Phys. Chem. C* **2015**, *119*, 4666−4674.

(11) Silvestri, L.; Forgia, S.; Farina, L.; Meggiolaro, D.; Panero, S.; La Barbera, A.; Brutti, S.; Reale, P. Lithium Alanates as Negative Electrodes in Lithium-Ion Batteries. *ChemElectroChem* **2015**, *2*, 877−886.

(12) Brown, H. C.; Krishnamurthy, S. Forty years of hydride reductions. *Tetrahedron* **1979**, *35*, 567−607.

(13) Aldridge, S.; Downs, A. J. *The Group 13 Metals Aluminium, Gallium, Indium and Thallium: Chemical Patterns and Peculiarities*; John Wiley & Sons, 2011.

(14) Brain, P. T.; Brown, H. E.; Downs, A. J.; Greene, T. M.; Johnsen, E.; Parsons, S.; Rankin, D. W. H.; Smart, B. A.; Tang, C. Y. Molecular structure of trimethylamine−gallane, $Me_3N{\cdot}GaH_3$: ab initio calculations, gas-phase electron diffraction and single-crystal X-ray diffraction studies. *J. Chem. Soc., Dalton Trans.* **1998**, 3685−3692.

(15) Calabro, M. Overview of Hybrid Propulsion. *Progress in Propulsion Physics* **2009**, *2*, 353−374.

(16) Schwartz, M. E.; Allen, L. C. Ab initio studies of the electronic structures of BH_3, BH_2F, BHF_2 and BF_3. *J. Am. Chem. Soc.* **1970**, *92*, 1466−1471.

(17) Carmichael, I. Ab initio configuration interaction study of the structure and magnetic properties of radicals and radical ions derived from group 13−15 trihydrides. *Chem. Phys.* **1987**, *116*, 351−367.

(18) Wickham-Jones, C. T.; Moran, S.; Ellison, G. B. Photoelectron spectroscopy of BH_3^-. *J. Chem. Phys.* **1989**, *90*, 795−806.

(19) Gutsev, G. L.; Bartlett, R. L. Electron affinity of CH_3 and BH_3 and the structure of their anions. *Polym. J. Chem.* **1998**, *72*, 1604−1614.

(20) Liu, Y.; Zhou, J.; Jena, P. Electronic Structure and Stability of Mono- and Bimetallic Borohydrides and Their Underlying Hydrogen-Storage Properties: A Cluster Study. *J. Phys. Chem. C* **2015**, *119*, 11056−11061.

(21) So, S. P. Ground electronic states and geometries of alane and its radical anion. *J. Mol. Struct.* **1977**, *39*, 127−131.

(22) Cramer, C. J. Calculation of the Electronic Structures and Spectra of Several Organic and Inorganic Radicals Containing Aluminum. *J. Mol. Struct.: THEOCHEM* **1991**, *235*, 243−262.

https://dx.doi.org/10.1021/acs.jpca.0c03432
J. Phys. Chem. A 2020, 124, 5369−5377

(23) Brzeski, J.; Czapla, M.; Skurski, P.; Simons, J. Selected boron, aluminum, and gallium trihalide and trihydride anions. *Chem. Phys.* **2017**, *482*, 387−392.
(24) Anusiewicz, I.; Skurski, P. Attaching Be or Mg to BH_3 results in the formation of $BeBH_3$ and $MgBH_3$ molecules capable of forming stable anions. *Chem. Phys. Lett.* **2018**, *698*, 19−23.
(25) Kalcher, J.; Sax, A. F. Gas Phase Stabilities of Small Anions: Theory and Experiment in Cooperation. *Chem. Rev.* **1994**, *94*, 2291−2318.
(26) Cížek, J. In *Advances in Chemical Physics*; Hariharan, P. C., Ed.; Wiley Interscience: New York, 1969, Vol. *14*, 35.
(27) Bartlett, R. J.; Purvis, G. D., III Many-body perturbation theory, coupled-pair many-electron theory, and the importance of quadruple excitations for the correlation problem. *Int. J. Quantum Chem.* **1978**, *14*, 561−581.
(28) Purvis, G. D., III; Bartlett, R. J. A full coupled-cluster singles and doubles model: The inclusion of disconnected triples. *J. Chem. Phys.* **1982**, *76*, 1910−1918.
(29) Scuseria, G. E.; Janssen, C. L.; Schaefer, H. F., III An efficient reformulation of the closed-shell coupled cluster single and double excitation (CCSD) equations. *J. Chem. Phys.* **1988**, *89*, 7382−7387.
(30) Kendall, R. A.; Dunning, T. H., Jr.; Harrison, R. J. Electron affinities of the first-row atoms revisited. Systematic basis sets and wave functions. *J. Chem. Phys.* **1992**, *96*, 6796−6806.
(31) Hill, J. G.; Peterson, K. A. Gaussian basis sets for use in correlated molecular calculations. XI. Pseudopotential-based and all-electron relativistic basis sets for alkali metal (K−Fr) and alkaline earth (Ca−Ra) elements. *J. Chem. Phys.* **2017**, *147*, 244106.
(32) Zakrzewski, V. G.; Ortiz, J. V.; Nichols, J. A.; Heryadi, D.; Yeager, D. L.; Golab, J. T. Comparison of Perturbative and Multiconfigurational Electron Propagator Methods. *Int. J. Quantum Chem.* **1996**, *60*, 29−36.
(33) Simons, J. Direct Calculation of First- and Second-Order Density Matrices. The Higher RPA Method. *J. Chem. Phys.* **1971**, *55*, 1218−1230.
(34) Ortiz, J. V. Electron Binding Energies of Anionic Alkali Metal Atoms from Partial Fourth Order Electron Propagator Theory Calculations. *J. Chem. Phys.* **1988**, *89*, 6348−6352.
(35) Rowe, D. J. Equations-of-Motion Method and the Extended Shell Model. *Rev. Mod. Phys.* **1968**, *40*, 153−166.
(36) Cederbaum, L. S. One-body Green's function for atoms and molecules: theory and application. *J. Phys. B: At. Mol. Phys.* **1975**, *8*, 290−303.
(37) Simons, J. Energy-shift Theory of Low-Lying Excited Electronic States of Molecules. *J. Chem. Phys.* **1972**, *57*, 3787−3792.
(38) Simons, J.; Smith, W. D. Theory of Electron Affinities of Small Molecules. *J. Chem. Phys.* **1973**, *58*, 4899−4907.
(39) Zakrzewski, V. G.; Ortiz, J. V. Semidirect Algorithms for Third Order Electron Propagator Calculations. *Int. J. Quantum Chem.* **1995**, *53*, 583−590.
(40) Zakrzewski, V. G.; Ortiz, J. V. Semidirect Algorithms in Electron Propagator Calculations. *Int. J. Quantum Chem.* **1994**, *52*, 23−27.
(41) Zakrzewski, V. G.; Dolgounitcheva, O.; Ortiz, J. V. Ionization Energies of Anthracene, Phenanthrene, and Naphthacene. *J. Chem. Phys.* **1996**, *105*, 8748−8753.
(42) Foster, J. P.; Weinhold, F. Natural hybrid orbitals. *J. Am. Chem. Soc.* **1980**, *102*, 7211−7218.
(43) Reed, A. E.; Weinhold, F. Natural bond orbital analysis of near-Hartree−Fock water dimer. *J. Chem. Phys.* **1983**, *78*, 4066−4073.
(44) Reed, A. E.; Weinstock, R. B.; Weinhold, F. Natural population analysis. *J. Chem. Phys.* **1985**, *83*, 735−746.
(45) Carpenter, J. E.; Weinhold, F. Analysis of the geometry of the hydroxymethyl radical by the "different hybrids for different spins" natural bond orbital procedure. *J. Mol. Struct.: THEOCHEM* **1988**, *169*, 41−62.
(46) Reed, A. E.; Curtiss, L. A.; Weinhold, F. Intermolecular interactions from a natural bond orbital, donor-acceptor viewpoint. *Chem. Rev.* **1988**, *88*, 899−926.
(47) Frisch, M. J.; Trucks, G. W.; Schlegel, H. B.; Scuseria, G. E.; Robb, M. A.; Cheeseman, J. R.; Scalmani, G.; Barone, V.; Petersson, G. A.; Nakatsuji, H.; et al. *Gaussian 16*, Revision C.01; Gaussian, Inc.: Wallingford, CT, 2016.
(48) Cordero, B.; Verónica Gómez, V.; Ana E. Platero-Prats, A. E.; Revés, M.; Echeverría, J.; Cremades, E.; Barragán, F.; Alvarez, S. Covalent Radii Revisited. *Dalton Trans.* **2008**, 2832−2838.
(49) Sawicka, A.; Anusiewicz, I.; Skurski, P.; Simons, J. Dipole-Bound Anions Supported by Charge-Transfer Interaction: Anionic States of $H_nF_{3-n}N{\rightarrow}BH_3$ and $H_3N{\rightarrow}BH_nF_{3-n}$ (n = 0, 1, 2, 3). *Int. J. Quantum Chem.* **2003**, *92*, 367−375.
(50) Miller, T. M.; Leopold, D. G.; Murray, K. K.; Lineberger, W. C. Electron affinities of the alkali halides and the structure of their negative ions. *J. Chem. Phys.* **1986**, *85*, 2368−2375.

https://dx.doi.org/10.1021/acs.jpca.0c03432
J. Phys. Chem. A 2020, 124, 5369−5377